

Photocatalytic degradation of malonic acid in aqueous suspensions of titanium dioxide: an initial kinetic investigation of CO₂ photogeneration

Yüksel İnel, Ayşe Neren Ökte

Department of Chemistry, Boğaziçi University, Bebek 80815, Istanbul, Turkey

Received 17 August 1995; accepted 27 November 1995

Abstract

The photocatalytic oxidation of malonic acid in aqueous suspensions of TiO₂ was investigated by following the formation of CO₂. The rate of formation of CO₂ is affected by the pH of the aqueous suspension, TiO₂ loading, malonic acid concentration, temperature, irradiation time, flow rate and light intensity. The disappearance of malonic acid fits a Langmuir–Hinshelwood kinetic model. Rate constants were calculated by including a correction term $\alpha(T)$ to take into account the decrease in the solubility of CO₂ with increasing temperature. The activation energy is 9.99 kJ mol⁻¹. A quantum yield of 0.26 for CO₂ formation was estimated from the proposed mechanism.

Keywords: Photocatalytic degradation; Malonic acid; TiO₂; CO₂

1. Introduction

In recent years, TiO₂ suspended in aerated water has been proven to be the most active photocatalyst with a band gap of 3.2 eV. The absorption of light with an energy greater than that of the band gap generates electron–hole pairs and subsequent oxidation–reduction processes.

So far, extensive work has shown that many organic compounds in aqueous solutions containing near-UV-illuminated suspensions of TiO₂ are oxidized completely to CO₂ [1]. In this work, we report a recent investigation of the photocatalytic oxidation of malonic acid (HOOC–CH₂–COOH), a representative member of the dicarboxylic acid family, in the presence of TiO₂. The possible photocatalytic oxidation of this compound to give CO₂ was followed and the initial kinetics of CO₂ photogeneration were studied. The disappearance of the acid and the formation of intermediate products were not analysed. In order to understand the mechanism of CO₂ formation, the effects of various factors, such as the catalyst concentration, flow rate, pH, concentration of malonic acid, temperature, irradiation time and light intensity, were investigated.

2. Experimental details

2.1. Materials

Degussa P25 grade titanium dioxide was a generous gift from Degussa Ltd., Turkey. It has a BET surface area of

50 ± 15 m² g⁻¹ and an average particle size of 30 nm. X-Ray diffraction analysis showed that this material was mostly in the anatase form.

All chemicals used in the experiments were of laboratory reagent grade and were used without further purification.

2.2. The photochemical reactor

The experiments were carried out in a gas recycling reactor made of a Pyrex tube (length, 36.2 cm; outer diameter, 13 cm; inner diameter, 3.5 cm). It contained an inner glass tube with a thickness of 2 cm. The temperature of the system was controlled by a Julabo F40 Ultratemp 2000 water circulator connected to the inner glass tube. The suspension was contained in the annulus between the two tubes. The gas above the suspension was pumped using a Cole–Parmer peristaltic pump. A sintered glass disc, placed at the bottom of the reactor, provided for the circulation of air and prevented the settlement of the suspension. Tygon tubing was used for the connections. The reactor was placed in an irradiation box (length, 70 cm; width, 22 cm). Six 20 W black light fluorescent lamps (General Electric F 20 T 12/BLB) were used. Two together were attached to the right- and left-hand sides and the back of the box. It was possible to light them one by one. The front side of the box was designed to operate as a door and the reactor was attached to the front side in order to maintain a uniform geometry throughout the experiments. A fan was placed at the top of the box and air was continually

circulated through the box in order to eliminate the heating effect of the lamps.

For most of the experiments described in this paper, stock solutions of malonic acid were prepared as 1×10^{-3} M at the natural pH (pH 3.4). The reaction mixture (200 ml) was mixed with the catalyst TiO_2 (1 g l^{-1}). A sonicator was used to ensure the uniform mixing of the TiO_2 suspension before mixing with malonic acid. Solutions were wrapped with Al foil and kept in the dark in order to prevent any interference from surrounding light before irradiation. The pH values of the reaction solutions were adjusted by adding HClO_4 or NaOH.

2.3. Analyses

A heated gas sampler (Shimadzu type HGS-2) was used to pass the gas samples into the gas chromatograph (GC) (Gow Mac). A GC equipped with a Porapak-N packed column and a thermal conductivity detector was used. The carrier gas was helium with a flow rate of 60 ml min^{-1} .

Calibrations were carried out using measured volumes of carbon dioxide added to the circulating gas phase loop under identical conditions with the experiments.

3. Results and discussion

3.1. Effect of catalyst concentration and flow rate

The dependence of CO_2 formation on the TiO_2 concentration was followed in the range $0.1\text{--}3.1 \text{ g l}^{-1}$ (Table 1). Each point in Fig. 1 shows the result for 1 h irradiation. CO_2 formation increases with increasing TiO_2 concentration up to 0.8 g l^{-1} . With a further increase in TiO_2 concentration, the formation of CO_2 appears to reach a limiting value, representing the contribution of two main factors. One factor is the aggregation of TiO_2 particles at high concentrations, causing a decrease in the number of surface active sites. The other is that higher catalyst concentrations, because of the opacity and light scattering properties of the particles, can lead to a decrease in the passage of irradiation through the sample. Thus 1 g l^{-1} TiO_2 was chosen (near the beginning of the plateau) for further experiments.

The inset in Fig. 1 shows the results of CO_2 formation as a function of flow rate. Experiments were carried out at three different flow rates (Table 2). Although less CO_2 was formed at low flow rates, 288 ml min^{-1} was used in order to prevent the overflow of the solution from the reactor and escape to the Tygon tubing which passes through the peristaltic pump.

3.2. Effect of pH

The formation of CO_2 was determined as a function of the solution pH in the range pH 1.7–9. The results are plotted in Fig. 2.

Table 1
Effect of TiO_2 loading on CO_2 formation

TiO_2 (g l^{-1})	CO_2 (μmol)
0.1	0.66
0.2	1.6
0.3	1.6
0.7	2.3
1.4	2.4
2.1	2.3
3.1	2.2

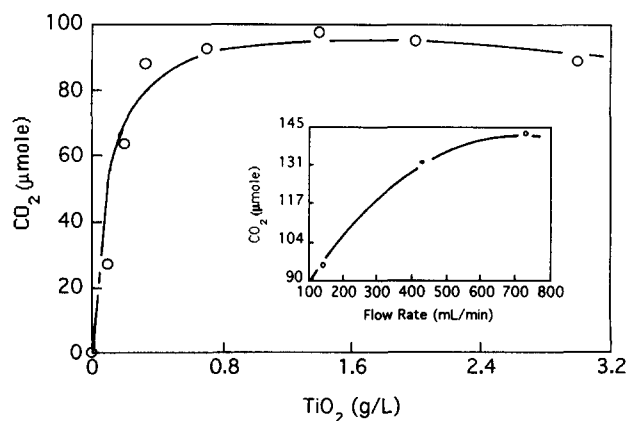


Fig. 1. Effect of the amount of TiO_2 on the formation of CO_2 . The inset shows CO_2 formation as a function of the flow rate.

Table 2
Effect of flow rate on CO_2 formation

Flow rate (ml min^{-1})	CO_2 (μmol)
144	95.3
432	132
720	143

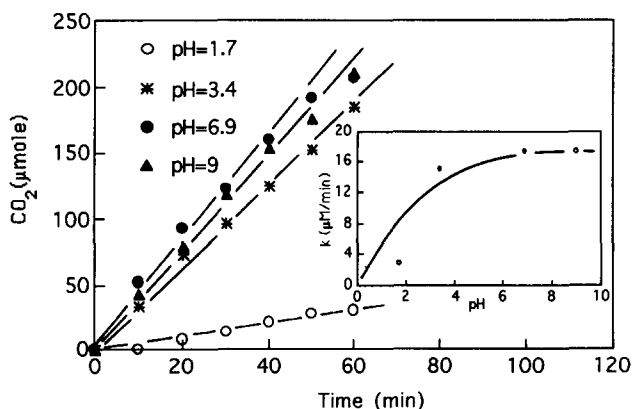


Fig. 2. Evolution of CO_2 at different pH values. The inset shows the effect of pH on the rate of CO_2 formation. Conditions: [malonic acid] = 1×10^{-3} M, $T = 294 \text{ K}$, intensity = $1.8 \times 10^{-7} \text{ einstein s}^{-1}$, [TiO_2] = 1 g l^{-1} , flow rate = 288 ml min^{-1} .

The ionizable hydrogens of malonic acid can be abstracted according to the $\text{p}K_1$ (2.85) and $\text{p}K_2$ (5.69) values [2]. The

Table 3
Effect of pH on the rate of CO₂ formation

k ($\mu\text{M min}^{-1}$)	pH
2.86	1.7
15.1	3.4
17.3	6.9
17.4	9.0

Following results (Table 3) were obtained when the rates of CO₂ formation were plotted against pH.

- 1) When the pH of the medium is below pK_1 , the rate of formation of CO₂ is at its lowest. This can be explained by the presence of acid in its acidic form (i.e. no hydrogen is lost) which obstructs the formation of CO₂.
- 2) There is a small difference between the natural pH of the acid and its pK_1 value. Therefore, one of the hydrogens can be lost, enhancing the rate of CO₂ formation.
- 3) At $\text{pH} \approx 7$, both ionizable hydrogens are abstracted, leading to the effective formation of CO₂.
- 4) The surface charge of TiO₂ is strongly influenced by the pH. The isoelectric point for TiO₂ in water is pH 6. At lower pH values, a positive surface charge is expected, and at higher pH values, a negative surface charge. At pH 9, the surface of TiO₂ will therefore be negatively charged. In addition, malonic acid exists in its dianionic form. Under these conditions, the predominant effect may lead to a decrease in the rate of CO₂ production. However, the decrease in CO₂ production does not occur to an appreciable extent. This implies that hydroxyl radicals may diffuse into the solution and react with malonic acid molecules.

3.3. Effect of irradiation time

The yield of CO₂ from 200 ml solutions of 1×10^{-3} M malonic acid at its natural pH, containing 0.2 g of TiO₂, was followed to extended irradiation times (Table 4) and, after irradiation for 150 min, the formation of CO₂ reached a plateau (Fig. 3).

Table 4
Effect of irradiation time on CO₂ formation

Time (min)	CO ₂ (μmol)
0	0
10	33.2
20	73.1
30	96.2
40	124
50	152
60	185
80	217
100	260
120	289
140	320
160	320

A linear increase in the formation of CO₂ was observed during the first 60 min (Fig. 3, inset). Therefore, to compare different results and to shorten the duration of the experiments, we measured CO₂ formation for 60 min in all cases.

3.4. Effect of acid concentration

The effect of concentration on CO₂ formation was investigated in the $(0.01-1) \times 10^{-3}$ M range by using slurries at natural pH and at a constant temperature of 21 °C. The rate of formation of CO₂ was assumed to be equal to the rate of disappearance of malonic acid for the examination of the effect of acid concentration on the CO₂ yield.

Fig. 4 shows the amount of CO₂ evolved, which increases linearly with the concentration of malonic acid.

The formation of CO₂ reaches a plateau in Fig. 5, indicating that the photogeneration of CO₂ obeys zero-order kinetics. The Langmuir–Hinshelwood (LH) model also holds for malonic acid (Fig. 5, inset); the rate expression can be written as

$$R = dC/dt = k(KC) / 1 + KC$$

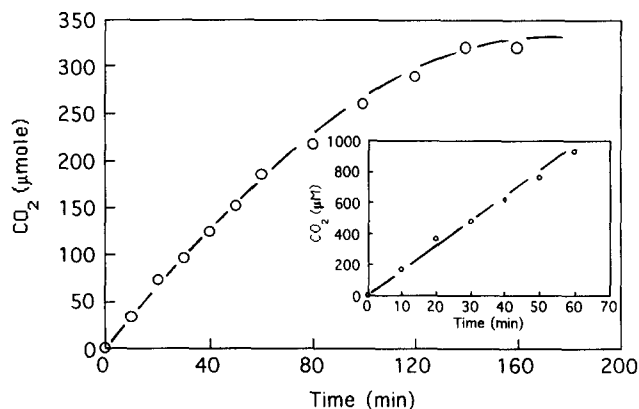


Fig. 3. Effect of irradiation time on CO₂ evolution. The inset shows the rate of CO₂ formation after 60 min irradiation time. Conditions: pH 3.4 (natural), [malonic acid] = 1×10^{-3} M, $T = 294$ K, intensity = 1.8×10^{-7} einstein s^{-1} , [TiO₂] = 1 g l^{-1} , flow rate = 288 ml min^{-1} .

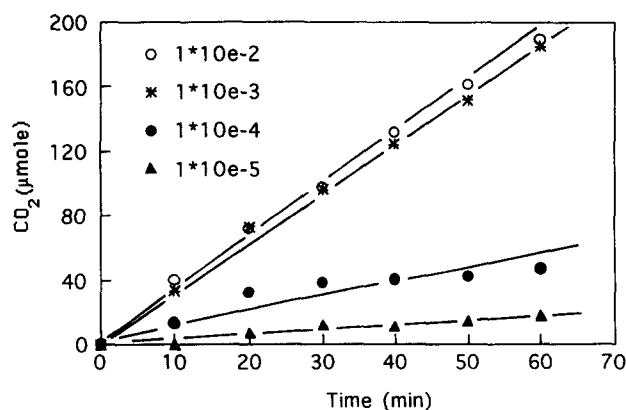


Fig. 4. The evolution of CO₂ as a function of malonic acid concentration. Conditions: pH 3.4 (natural), $T = 294$ K, intensity = 1.8×10^{-7} einstein s^{-1} , [TiO₂] = 1 g l^{-1} , flow rate = 288 ml min^{-1} .

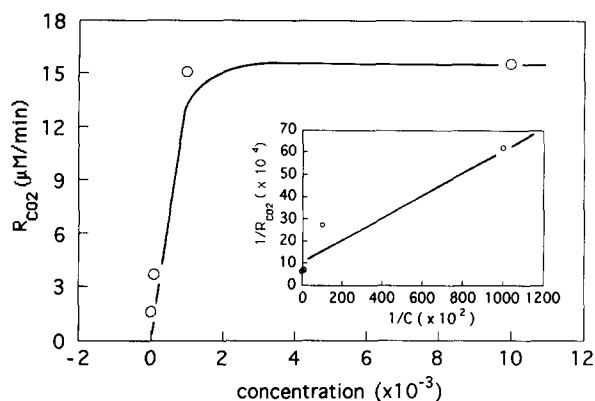


Fig. 5. Rate of CO₂ formation vs. malonic acid concentration. The inset shows $1/R_{\text{CO}_2}$ vs. $1/C$.

Table 5
Effect of malonic acid concentration on the rate of CO₂ formation

R_{CO_2} ($\mu\text{M min}^{-1}$)	C (M) ($\times 10^{-3}$)	$1/R_{\text{CO}_2}$ (min M^{-1}) ($\times 10^4$)	$1/C$ (M^{-1}) ($\times 10^2$)
15.5	10	6.45	1
15.1	1.0	6.67	10
3.69	0.1	27.1	100
1.61	0.01	62.1	1000

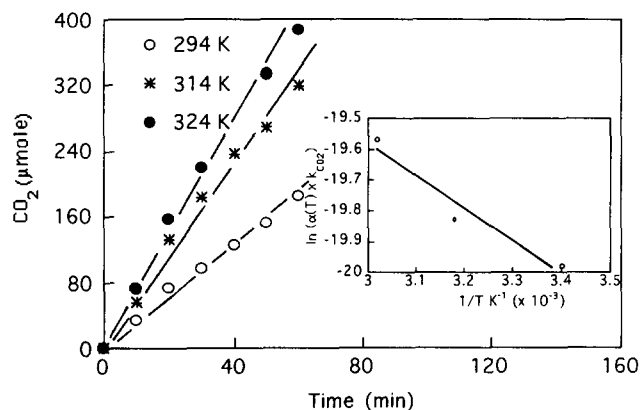


Fig. 6. The evolution of CO₂ at various temperatures. The inset shows an Arrhenius plot. Conditions: pH 3.4 (natural), [malonic acid] = 1×10^{-3} M, intensity = 1.8×10^{-7} einstein s⁻¹, [TiO₂] = 1 g l⁻¹, flow rate = 288 ml min⁻¹.

Table 6
Arrhenius data for malonic acid

$\ln[\alpha(T) \times k_{\text{CO}_2}]$	$1/T$ (K ⁻¹) ($\times 10^{-3}$)
-19.98	3.401
-19.83	3.181
-19.57	3.091

where C is the concentration of the acid, k is the reaction rate constant ($8.97 \mu\text{M min}^{-1}$) and K is the adsorption equilibrium constant ($0.0214 \mu\text{M}^{-1}$). The linearity of a plot of $1/R$ vs. $1/C$, where $1/k$ is the intercept and $1/kK$ is the slope, indicates that the LH model is valid [3]. The validity of the

LH model confirms that the photo-oxidation occurs completely on the TiO₂ surface. The results are shown in Table 5.

3.5. Effect of temperature

The variation in CO₂ formation was followed at three different temperatures (21, 41 and 51 °C); it is found that increasing the temperature increases the reaction rate (Fig. 6). A correction term $\alpha(T)$ is needed to take into account the decrease in the solubility of CO₂ with increasing temperature. The temporal variation in the total number of moles of CO₂ ($N(\text{CO}_2)$) can be determined using the formula [4]

$$N(\text{CO}_2) = [\text{CO}_2] (V_{\text{HS}}/V + V_{\text{LP}}K_{\text{CO}_2}T/294) / 100 \\ = \alpha(T) [\text{CO}_2]$$

where V_{HS} is the volume of the head space (0.150 l), V is the volume of one mole of gas at $T = 21$ °C and $P = 1$ atm (24.1 l), V_{LP} is the volume of the liquid phase (0.200 l) and K_{CO_2} is the equilibrium constant for the process $\text{CO}_2(\text{g}) \rightleftharpoons \text{CO}_2(\text{aq})$ and is equal to $3.9 \times 10^{-2} \text{ mol l}^{-1} \text{ atm}^{-1}$ at 21 °C [5].

In this study, most of the experiments were carried out at $T = 21$ °C, and therefore $\alpha(T)$ is $14.02 \times 10^{-5} \text{ mol}/[\text{CO}_2]$. At 41 °C, $\alpha(T)$ is $10.74 \times 10^{-5} \text{ mol}/[\text{CO}_2]$, and at 51 °C, $\alpha(T)$ is $9.83 \times 10^{-5} \text{ mol}/[\text{CO}_2]$.

The Arrhenius plot ($\ln[\alpha(T) \times k_{\text{CO}_2}]$ vs. $1/T$) (Table 6) is shown in the inset of Fig. 6; the slope leads to the calculation of the activation energy as 9.99 kJ mol⁻¹.

3.6. Effect of light intensity

CO₂ formation from malonic acid was also investigated as a function of the light intensity. The light intensity was measured using a potassium ferrioxalate actinometer and was found to be 0.3×10^{-7} einstein s⁻¹ in the wavelength region 300–400 nm. When the light intensity was increased, higher CO₂ formation was observed (Fig. 7).

When the reaction rates were plotted against the intensities of the lamps, no linear correlation was observed (Fig. 8);

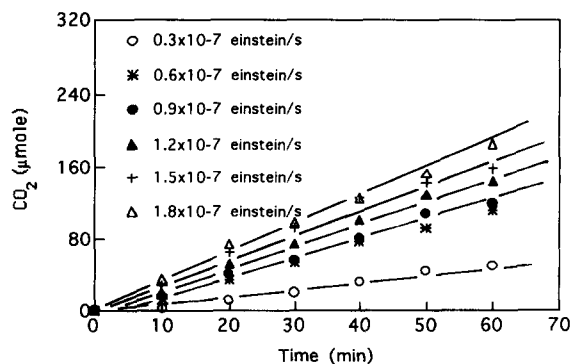


Fig. 7. CO₂ formation as a function of the lamp intensity. Conditions: pH 3.4 (natural), [malonic acid] = 1×10^{-3} M, $T = 294$ K, [TiO₂] = 1 g l⁻¹, flow rate = 288 ml min⁻¹.

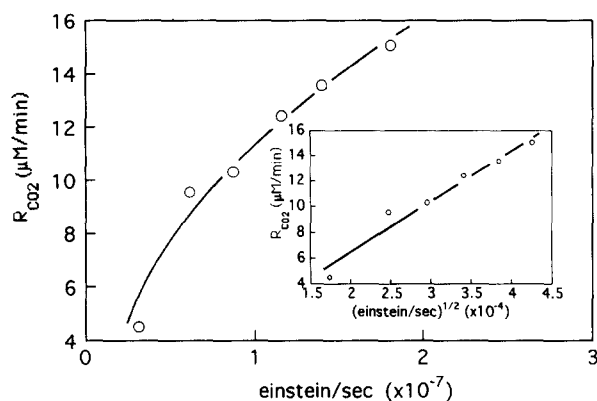


Fig. 8. Effect of light intensity on the rate of CO₂ formation. The inset shows the effect of the square root of light intensity on CO₂ evolution.

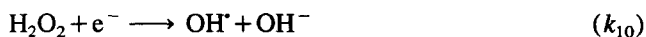
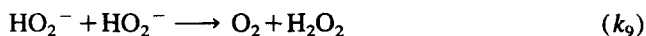
Table 7
Effect of light intensity on the rate of CO₂ formation

R_{CO_2} $\mu M \text{ min}^{-1}$	Intensity (einstein s^{-1}) ($\times 10^{-7}$)	Intensity ^{1/2} (einstein s^{-1}) ^{1/2} ($\times 10^{-4}$)
4.51	0.3	1.73
9.54	0.6	2.45
10.3	0.9	3.00
12.4	1.2	3.46
13.5	1.5	3.87
15.1	1.8	4.24

however, a straight line was obtained when the square root of the intensity of the lamps was plotted (inset in Fig. 8). These results, also given in Table 7, can be explained in terms of the increased importance of electron-hole recombination at higher light intensities.

3.7. Postulated mechanism

The proposed reactions involved in the photo-oxidation of malonic acid (MA, malonic acid) were given as input to a program written in Fortran in IBM. The following mechanism can be proposed.



$$d[\text{TiO}_2]/dt = -k_1[\text{TiO}_2](h\nu) = \Phi I$$

$$d(e^-)/dt = -k_6[\text{H}^+](e^-) - k_7[\text{O}_2](e^-) - k_{10}[\text{H}_2\text{O}_2](e^-) + k_1[\text{TiO}_2](h\nu)$$

$$d(h^+)/dt = -k_4[\text{MA}^-](h^+) + k_1[\text{TiO}_2](h\nu)$$

$$d[\text{MA}]/dt = -k_2[\text{MA}] - k_{11}[\text{MA}][\text{OH}^*] + k_3[\text{MA}^-][\text{H}^+]$$

$$d[\text{MA}^-]/dt = -k_3[\text{MA}^-][\text{H}^+] - k_4[\text{MA}^-](h^+) + k_2[\text{MA}]$$

$$d[\text{H}^+]/dt = -k_3[\text{MA}^-][\text{H}^+] - k_6[\text{H}^+](e^-) + k_2[\text{MA}]$$

$$d[\text{MA}^*]/dt = -k_5[\text{MA}^*] + k_4[\text{MA}^-](h^+)$$

$$d[\text{R}^*]/dt = -k_{12}[\text{R}^*][\text{H}^+] + k_5[\text{MA}^*] + k_{11}[\text{MA}][\text{OH}^*]$$

$$d[\text{CO}_2]/dt = k_5[\text{MA}^*]$$

$$d[\text{H}^*]/dt = -k_8[\text{O}_2^{\bullet -}][\text{H}^*] - k_{12}[\text{R}^*][\text{H}^+] + k_6[\text{H}^+](e^-)$$

$$d[\text{O}_2]/dt = -k_7[\text{O}_2](e^-) + k_9[\text{HO}_2^-][\text{HO}_2^-]$$

$$d[\text{O}_2^{\bullet -}]/dt = -k_8[\text{O}_2^{\bullet -}][\text{H}^*] + k_7[\text{O}_2](e^-)$$

$$d[\text{HO}_2^-]/dt = -2k_9[\text{HO}_2^-][\text{HO}_2^-] + k_8[\text{O}_2^{\bullet -}][\text{H}^*]$$

$$d[\text{H}_2\text{O}_2]/dt = -k_{10}[\text{H}_2\text{O}_2](e^-) + k_9[\text{HO}_2^-][\text{HO}_2^-]$$

$$d[\text{OH}^*]/dt = -k_{11}[\text{MA}][\text{OH}^*] + k_{10}[\text{H}_2\text{O}_2](e^-)$$

$$d[\text{OH}^-]/dt = k_{10}[\text{H}_2\text{O}_2](e^-)$$

$$d[\text{H}_2\text{O}]/dt = k_{11}[\text{MA}][\text{OH}^*]$$

$$d[\text{TH}]/dt = k_{12}[\text{R}^*][\text{H}^*]$$

As a result, the CO₂ formation rate and quantum yield can be calculated as

$$R_{CO_2} = d[\text{CO}_2]/dt = \Phi I$$

where Φ is the quantum yield and I is the intensity; the overall quantum yield was found to be 0.26.

4. Conclusions

Our experimental results indicate that the rate of formation of CO₂ is pH dependent. The Langmuir-type plot obtained

confirms that the photo-oxidation reaction takes place on the surface of TiO₂. Taking into consideration the observation that an increase in temperature leads to a significant increase in the rate of CO₂ formation, the activation energy can be calculated as 9.99 kJ mol⁻¹. By increasing the number of lamps, the rate of CO₂ formation increases linearly. However, it should be noted that, at high intensities, the probability of electron–hole recombination also increases, which inhibits this linearity. In this case, the rate of CO₂ formation vs. the square root of intensity can be plotted as a straight line. The rate of CO₂ formation increases with increasing irradiation time; however, a limit is observed after 150 min when the formation of CO₂ reaches a plateau.

Acknowledgements

This research was supported by the AVICENNE Research Programme of the European Community (Project No. 074).

References

- [1] R.W. Matthews, *Water Res.*, 20 (1986) 569.
- [2] R.T. Morrison and R.N. Boyd, *Organic Chemistry*, Allyn and Bacon Inc., Newton, MA, 1987, p. 846.
- [3] M.A. Fox and M.T. Dulay, *Chem. Rev.*, 93 (1993) 341.
- [4] A. Mills and S. Morris, *J. Photochem. Photobiol. A: Chem.*, 71 (1993) 75.
- [5] R.E. Loewenthal and G.R. Marais, *Carbonate Chemistry of Aquatic Systems: Theory and Application*, Ann Arbor, MI, 1976, p. 246.